SEVIRI SST Diurnal warming and QuikSCAT ocean Winds in the North Sea and the Baltic Sea

Karagali, Ioanna; Høyer, Jacob L.

Published in:
Proceedings

Publication date:
2010

SEVIRI SST DIURNAL WARMING & QUIKSCAT OCEAN WINDS IN THE NORTH SEA AND THE BALTIC SEA

Ioanna Karagali, Jacob L. Hoeyer

Risoe National Laboratory for Sustainable Energy,Technical University of Denmark,Roskilde,Denmark
Centre for Ocean and Ice, Danish Meteorological Institute, Copenhagen, Denmark

Abstract

A significant percentage of the incoming solar radiation is absorbed by the few top meters of the ocean surface. As a result an increase of the sea surface temperature occurs in a manner that depends on the daily solar cycle. Lack of wind prevents mixing of the water column, thus leading to the formation of a thermal layer on the top of the water column where the temperature is higher when compared with the one bellow and above. This phenomenon, known as diurnal warming, may typically start around 10:00 and last until 18:00 local solar time. It may temporarily affect air-sea interactions by altering the heat and gas fluxes, atmospheric circulation and the height of the atmospheric boundary layer.

Diurnal warming events in the North Sea and the Baltic Sea are investigated in terms of size, duration and magnitude of warming. Hourly measurements from the Spinning Enhanced Visible Infrared Imager (SEVIRI) instrument, on board the Meteosat Second Generation (MSG) satellites, are utilized to compute the daily anomaly fields, defined as hourly day-time measurements minus daily night-time reference fields. A basic sensitivity analysis concerning the night-time reference fields is performed since the magnitude of observed diurnal warming depends on the foundation temperature utilized to measure the anomalies. Additionally, wind speed measurements, available from the active microwave radar on board the QuikSCAT satellite are analyzed to examine the local wind regime prior, during and after the diurnal warming events. QuikSCAT provided coverage for the area of interest twice per day, i.e. at approximately 06:00 and 18:00. This does not satisfy the demand for high resolution wind vector information, required to capture wind speed variation during the diurnal warming events. Nonetheless, the long period of available QuikSCAT data provides a good reference as far as the frequency and spatial distribution of particularly low winds is concerned. Results indicate that the Baltic Sea and the eastern North Sea are areas where diurnal warming occurs during the summer months of each year. That coincides very well with areas where low wind speeds are persistent.

INTRODUCTION

Diurnal warming events of the upper ocean can occur under conditions of light winds and strong solar heating. A significant percentage of the incoming solar radiation is absorbed by the few top meters of the water column, thus increasing its temperature in a manner that depends on the daily solar insolation. Low wind speeds prevent mixing of the water column, resulting in the formation of a surface thermal layer. The temperature difference between night and day may exceed three degrees [Gentemann et al. (2008), Merchant et al. (2008)] depending on the location and environmental conditions. This variation has an impact on air-sea interactions, namely heat, moisture and gas exchange.

Diurnal warming of the surface layer was identified during early in-situ studies from Stommel et al. (1969) and Kaiser (1978). It has been observed in different areas of the global ocean including the Mediterranean [Deschamps & Frouin (1984), Merchant et al. (2008)], western North Atlantic [Cornillon & Stramma (1985), Stramma et al. (1986)], the Gulf of California (Ward, 2006) and the global ocean

[Stuart-Menteth et al. (2003), Gentemann & Minett (2008)] using combinations of in situ and satellite observations. Diurnal warming has been found to start as early as 08:00 local solar time and persist as long as late afternoon, reaching a maximum at 15:00 (Gentemann et al., 2003). The magnitude and spatial distribution of diurnal warming events depend on local conditions and are affected by wind, cloud coverage and water turbidity (Merchant et al., 2008). The occurrence of such events indicates the existence of a thermal layer on top of the water column, associated with large fluxes of heat between the ocean and the atmosphere. The Group for High Resolution Sea Surface Temperature (GHRSST) pointed out that the existence of this warm layer on top of the water column can complicate the assimilation of SST by ocean and atmospheric models and the derivation of atmospheric correction algorithms for satellite radiometers and SST data merging. Thus, "identification of diurnal warming events across the global ocean is required in order to improve our understanding of their spatial and temporal variability as well as their impact at daily, monthly, seasonal, annual and multi-annual time scales" (Donlon et al., 2007).

The present paper aims at examining the daily SST variation in terms of magnitude, spatial distribution, frequency of occurrence and combining it with information regarding the wind regime in the North Sea and the Baltic Sea. Results regarding SST are obtained using data from SEVIRI as it is characterized by high spatial resolution and high sampling frequency. Wind vector information from the SeaWinds scatterometer on board the QuikSCAT platform was preferred, due to the long record of data. Until present, there has been no extended study regarding diurnal warming in these areas. Thus, the aim is to contribute to the ongoing research regarding the diurnal variability of SST, by using an extensive dataset in order to resolve the conditions prior to the events, their magnitude, extend and frequency in the North Sea and Baltic Sea where so far information has been limited.

DATA AND METHODS

SEVIRI Sea Surface Temperature

The Spinning Enhanced Visible and Infra-red Imager (SEVIRI) is on board the Meteosat Second Generation (MSG, MSG-2) satellites launched in 2002 and 2005 respectively. As an infra-red instrument it has no cloud penetration skill. Being in geostationary orbit centred at zero degrees latitude and longitude and with a nominal resolution of 0.03 degrees it records information every 15 minutes, on a circular domain extending from 60^0 South to 60^0 North and from 60^0 West to 60^0 East. Measurements are averaged in hourly intervals and are gridded in a 0.05 degrees grid.

SEVIRI data were provided by the Centre de Meteorologie Spatiale (CMS), as an experimental product. The domain of interest was defined as a rectangular grid extending from 48^0 to 60^0 North and from 10^0 West to 30^0 East. The spatial resolution of SEVIRI at the domain of interest, ranged between six and nine km depending on the incidence angle. Each daily file included 24 hourly measurements of SST with quality flags for the retrievals, ranging from zero (bad) to five (excellent). Data from April 2004 to October 2009 were utilized, corresponding to 1979 calendar days, where only pixels with quality flag five were chosen. If every day, all 24 measurements where flagged with quality five, there would be 47496 available measurements for every grid cell. The maximum amount of quality five retrievals observed for an individual grid cell was 7083, corresponding to a maximum 14.8% data availability.

The SEVIRI data availability for the quality five flag is shown in Figure 1, where areas of high data availability include the Baltic Sea, the Danish straits, the sea of Kategat and the English channel. Data availability is significantly reduced in the North Atlantic and most coastal areas. The North Atlantic is expected to have frequent overcast conditions, while data availability in coastal areas may have been affected by the masking scheme implemented during processing. Below 50^0 North, the change in data availability compared to the surrounding areas is related with the implementation of the Saharan Dust Index (SDI) flagging scheme applied from 2006 (LeBorgne, personal comment, 2010).

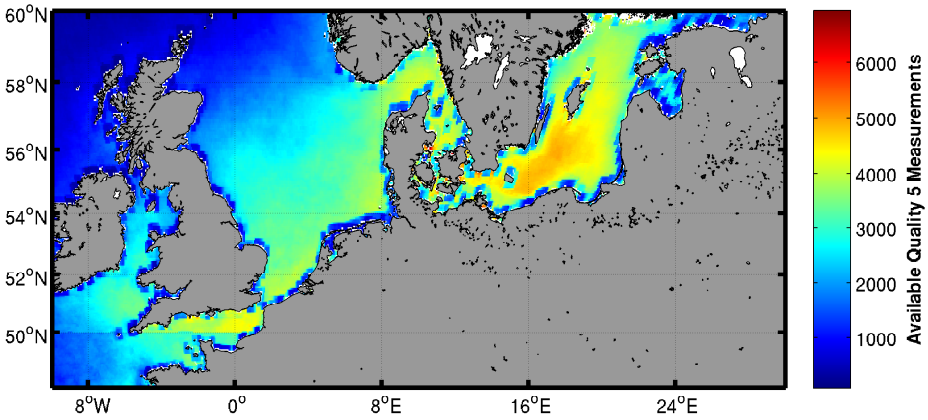

Figure 1: **Data availbility for SEVIRI, hourly SST measurements for the period June 2004-October 2009.**

QuikSCAT Ocean Vector Winds

QuikSCAT, launched by NASA in 1999, recorded ocean wind vector information until 2009.In sun-synchronous orbit at an altitude of 803 km, with a recurrent period of twice per day, and a wide swath of 1800 km it provided daily 90% coverage of the global ocean with resolution of 25 km. SeaWinds, the scatterometer on board the QuikSCAT platform, measured incoming radiation backscattered from the sea surface due to small scale waves, assumed to be in equilibrium with the wind (Hoffman & Leidner, 2005). For the purposes of the present study daily gridded data were obtained from Remote Sensing Systems (RSS) (www.remss.com), "produced daily by mapping the scatterometer orbital data to a 0.25 deg longitude by 0.25 deg latitude Earth grid". Each file includes wind speed and direction, local time of measurement, a scatterometer rain flag and a collocated radiometer rain flag. Due to the scatterometer's sensitivity to rain and the ambiguity it applied to the wind retrieval, all rain flags were utilized and quality control demanded that they indicated no rain for a grid cell measurement to be used for further analysis.

The period of investigation extended from April 2004 to October 2009, following the availability of SEVIRI data. The RSS product had 1975 days with available data, at least for one of the two modes which corresponds to 99.8% of the time. Grid cell information was used only if the rain quality control was successful. For a given grid cell, if both modes were free of rain for all 1975 days, there would potentially be 3950 available wind retrievals. The maximum amount of times that any given grid cell successfully completed the rain quality control was 3740, corresponding to a maximum of 94.7% data availability. The quality flags implemented for the RSS product were "scatflag" (0 for no rain) and the "radrain" corresponding to a collocated radiometer rain flag in [km*mm/hr] with values of zero corresponding to existing radiometer data that indicate no rain. Thus, in order to satisfy rain-free conditions, only data classified with "scatflag=0" and "radrain=0" or "radrain=-999" (no collocation available) were utilized for further analyses.

Night-time Reference Fields

Daily SST anomalies are defined as the exceedances over a threshold, i.e. the foundation temperature representative of the upper meters of the water column free of diurnal warming. Typical foundation temperatures occur under well mixed conditions when heat is uniformly distributed over the depth and are observed at night-time. In this paper the term "night-time reference field" is used to describe SST fields representative of foundation temperatures. As all diurnal warming events are influenced by the night-time reference field, the quality of it is essential and needs to be validated. Night-time reference fields were generated from the SEVIRI dataset, for every calendar day. As the instrument's observing ability is limited by clouds, overcast conditions reduced data availability. In order to overcome this, night-time measurements of the given day plus/minus a certain number of days were averaged. A sensitivity analysis was performed in order to define which would be the optimal night-time interval, how many days would be used for averaging and which quality flags would be selected. Moreover, an independent optimally interpolated SST product (Hoeyer & She, 2007) acquired from the Danish Meteorological Institute (DMI) was used for comparison.

The sensitivity analyses consisted of comparing a validation field and various night-time reference fields, generated utilising different sets of parameters, for a test period between April and December of 2006. The number of averaging days varied from one to five, the night-time interval extended form 22:00 to 06:00 with varying duration and quality flags varied from three to five. To evaluate the performance of the reference fields, the validation field was generated for every calendar day, by computing the local sunrise time and utilizing the last pre-dawn quality five measurement. Anomalies defined as the difference between validation fields and reference fields were estimated for this test period. Results were compared in terms of mean values and standard deviations along with data availability. It was decided to generate the night-time reference fields for every calendar day, using the temperature fields between 00:00 and 03:00 of the three calendar days prior and after the given day, accounting only for pixels flagged with qualities from three to five. All times refer to local time for any given location.

RESULTS

Night-Time Reference Fields

The distribution of data availability for the different reference fields (not shown here) showed that the amount of pixels ranged from 0 to 70000. The maximum possible water pixels included in the domain are 74645 for one daily reference field. The reference field generated only using quality five data showed the lowest data availability and little improvement, therefore it was excluded from further analysis. Reference fields where the “night-time” period was six hours long (from 22:00 to 04:00 or from 00:00 to 06:00) showed higher data availability more often than the ones where the “night-time” period was three (00:00 to 03:00) or four hours (00:00 to 04:00) long. The DMI-OI product always had the maximum amount of available data since it is an interpolated product with no gaps.

The distribution of mean anomalies, defined as “validation field – reference field”, is presented in terms of normalized counts during the test period, in Figure 2. Most frequently observed anomalies for all reference fields were either zero or negative, thus indicating that the reference fields were warmer than the validation field. Large negative anomalies were mainly observed for the DMI-OI product, which is based on multi-sensor infra-red and microwave night-time observations. Zero mean anomalies were most frequently observed for the reference field with nigh-time measurements from 00:00 to 06:00 and pixels with quality three to five. For this case, the night-time interval was extended enough to include the pre-dawn values used for the validation field, hence the zero difference. Reference fields with night-time intervals that extended to 04:00 local solar time showed frequently zero anomalies, explained by the fact that during spring and summer months the sunrise time in these latitudes may be as early as 03:30 local times. The reference field extending from 00:00 to 03:00 had most frequently observed anomalies in the range of zero to -0.1 [K], even though night-time data utilized to generate it were always prior to local sunrise time at any grid cell for every season. Standard deviations, shown in Figure 3, ranged for the different reference fields. The DMI-OI product showed most frequently observed standard deviation in the range of 0.3 to 0.5 [K], while the reference field with the shortest night-time interval (00:00-03:00) indicated standard deviations between 0.2 and 0.4 [K], with maximum at 0.3 [K]. The reference fields with extended night-time intervals had most frequent average standard deviations of 0.3 [K].

SEVIRI Diurnal Warming

In order to estimate the magnitude of diurnal warming the day-time anomalies were calculated, based on the temperature difference between day and night. The night-time temperature corresponds to well mixed conditions when the distribution of heat, thus the temperature, is uniform in the upper meters of the water column. For every calendar day the night-time reference field was computed using SEVIRI night-time data, as previously described. Hourly anomalies were defined as day-time measurement minus the night-time reference field and were computed for every grid cell from 08:00 to 20:00 local solar time. Three different thresholds were defined with all anomalies larger than one, two or three degrees. Spatial and temporal distributions were estimated by counting the number of times, when a grid cell satisfied the criteria of excellent quality and anomaly greater than the defined threshold. Only grid cells with more than 365 quality five observations, corresponding to a year of one observation per day, were included in the analysis.

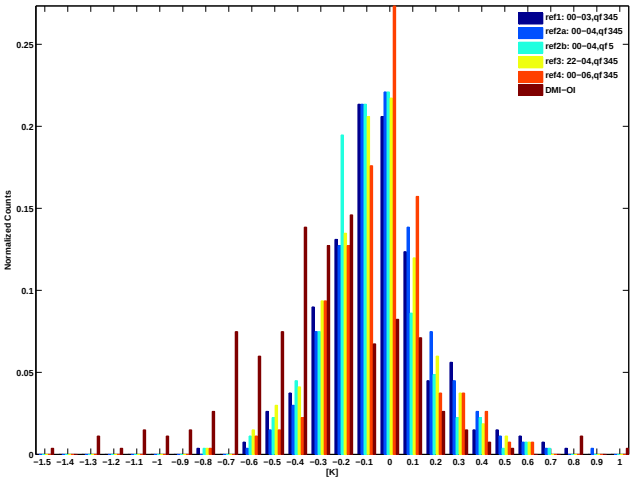

Figure 2: **Mean anomalies estimated as validation minus reference field for the test period (April-December 2006).**

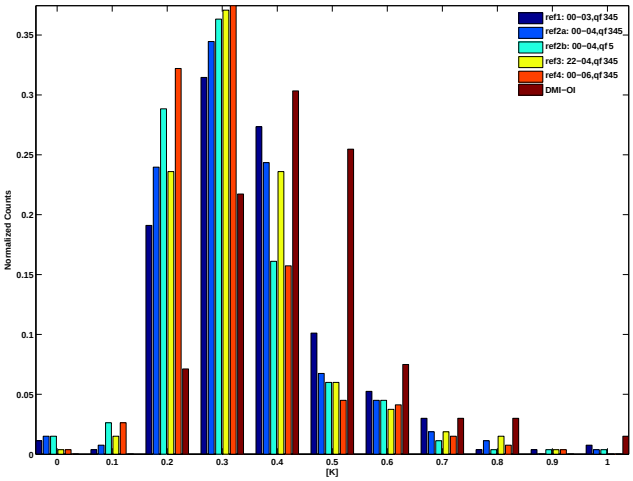

Figure 3: **Standard deviation of anomalies, estimated as validation minus reference field, for the test period (April-December 2006).**

The spatial distribution of diurnal warming exceeding two degrees is shown in Figure 4 as a percentage of the recorded quality five hourly measurements, thus in every grid cell the number of times when anomalies exceeded a given threshold was normalized with the amount of available data for the specific grid cell. Areas with most observations (5%) of anomalies larger than two degrees include the gulfs of Riga and Finland and the southern Baltic Sea. The Wadden Sea, Kattegat, Skagerrak, the Celtic Sea and the northern North Sea showed less frequent observations (3-5%). From the anomalies observed, 75% were not greater than 3 [K] but 5% of the cases exceeded 4.1 [K] (not shown). The distribution of anomalies throughout the day as a function of local solar time showed that anomalies larger than 3 [K] exhibited a narrow distribution, most frequently occurring between 13:00 and 17:00, with a maximum at 15:00. Duration of the events did not exceed four (three) hours for anomalies larger than one (three) degrees in 75% of the cases, while 5% of anomalies greater than one (three) degrees lasted more than eight (six) hours. Figure 6 shows the monthly distribution of anomalies exceeding different thresholds for the period June 2004 to October 2009. June and July are the prime months for diurnal warming larger than two degrees, followed by May and August.

QuikSCAT Winds

Analysis of scatterometer sea winds, retrieved from QuikSCAT, indicated that low wind speeds (< 3ms^{-1}), shown in Figure 5 as a percentage of rain-free observations were observed in the Celtic Sea, Skagerrak, the south Baltic Sea, Wadden Sea and the east coast of the British Isles. Maximum low wind observations were approximately 15% of the total rain-free observations, mainly occurring in the southern part of the Baltic Sea. Characteristic is the almost zero percentage of low wind observations in the central part

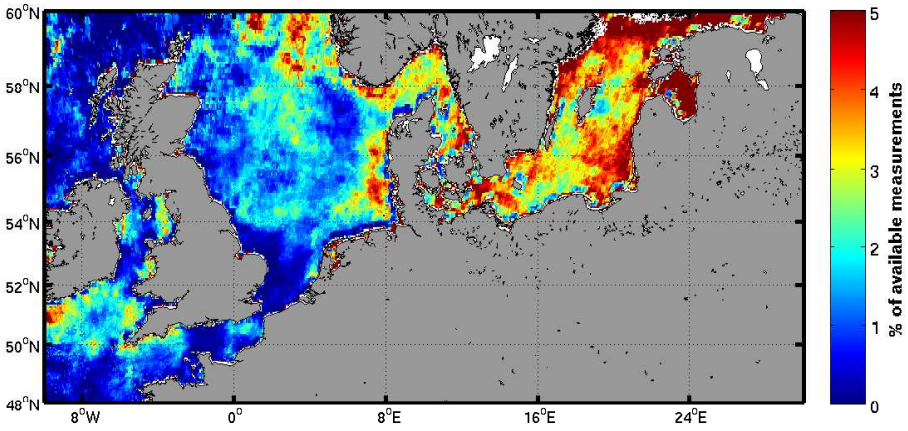

Figure 4: **Spatial distribution of anomalies greater than 2 [K] as percentage of available measurements, from June 2004 to October 2009.**

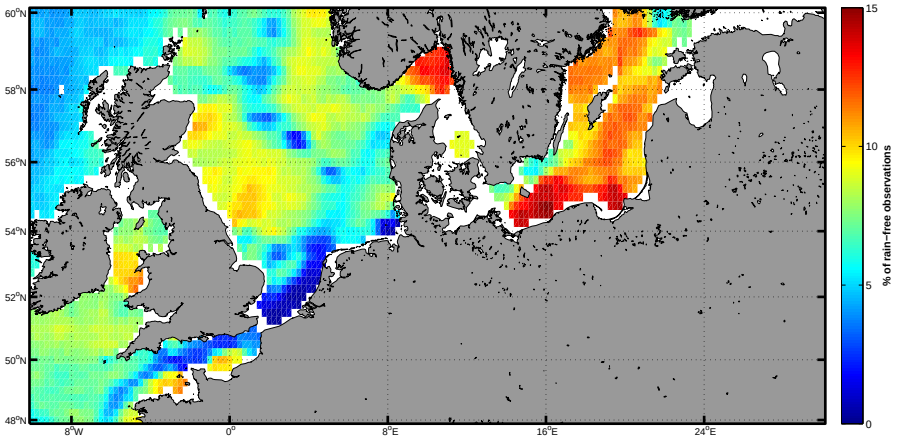

Figure 5: **Spatial distribution of wind speeds lower than 3ms^{-1} as percentage of rain-free measurements, from June 2004 to October 2009.**

of the North Sea and the English Channel. The annual distribution of QuikSCAT winds for the period June 2004 to October 2009, is shown Figure 7 for three different thresholds namely 3, 4 and 5ms^{-1} as normalized counts. Most cases with winds lower that 3ms^{-1} are observed during June, July and May. Winds lower than 5ms^{-1} tend to be more evenly distributed through the year, including late spring and early autumn months.

DISCUSSION

Diurnal warming of the sea surface temperature occurs during day-time under conditions of light winds and strong solar insolation. Day-time warming levels are defined given a known appropriate foundation temperature, representative of well mixed conditions. The representation of foundation temperature fields has been investigated using the operational OI product from DMI and night-time reference fields generated from the SEVIRI dataset. It has been shown that the statistical characteristics of the produced anomalies vary little with respect to the reference fields implemented. Therefore, it was chosen to continue the analysis utilizing the SEVIRI reference fields as they can be easily generated from the dataset itself and long term systematic sensor biases will not influence results of diurnal warming.

Data availability was limited for the areas of interest, with a maximum of 15% quality five observations over the period of investigation. As an infrared radiometer, SEVIRI cannot penetrate through clouds and since the North Sea is well positioned within the North hemisphere storm track, cloudy conditions are frequently observed. Despite that, the suspiciously low data availability observed in coastal areas demises the reliability of the applied flagging schemes. Thus, it is possible that good quality observations

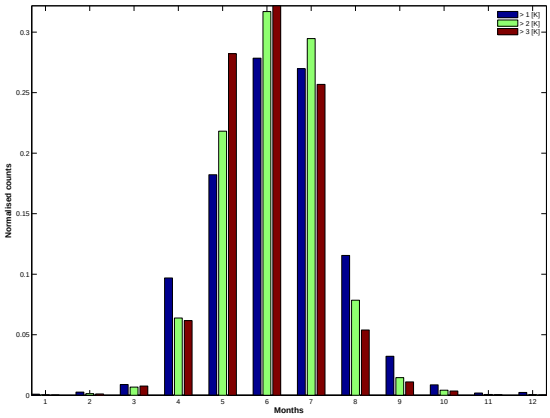

Figure 6: **Monthly distribution of anomalies exceeding thresholds of 1 (blue), 2 (green), 3 [K] (red), June 2004 to October 2009.**

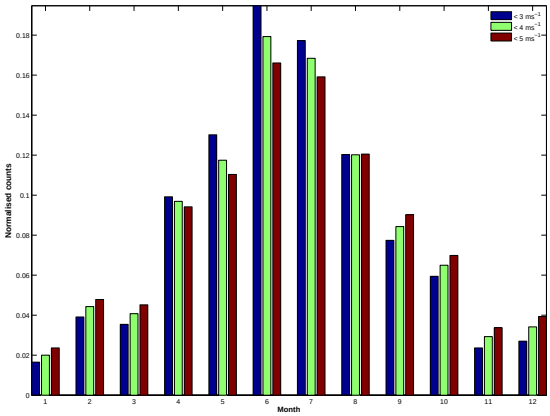

Figure 7: **Monthly distribution of winds lower than 3ms^{-1} (blue), 4ms^{-1} (green), 5ms^{-1} (red), June 2004 to October 2009.**

are discarded and the relatively low percentages of available measurements and observed anomalies should not be considered as an indicator that diurnal warming does not occur often in these areas.

Anomalies exceeding various thresholds were observed during late spring and early summer months of each year in areas where frequent low winds were observed in the same period. The peak time of occurrence for anomalies larger than three degrees was found at 15:00, in good agreement with observations from Gentemann et al. (2003). Their spatial distribution included the gulfs of Riga and Finland, the south Baltic Sea and the Danish straits, the Wadden Sea and the coast of Norway. Especially the areas in the Baltic Sea are semi-closed gulfs, surrounded by land with small depth and reduced circulation. Moreover, during the summer months the optical properties of the water are such that the penetration depth of light in the water column is approximately 3-5 meters (not shown here). Thus, it is believed that high water opacity in these areas holds an important role for diurnal warming (Merchant et al., 2008).

Low winds were observed mainly during spring, summer and early autumn in areas well corresponding to those of diurnal warming. The mission description allowed wind speed measurements in the range 3-20 ms^{-1} with an accuracy of 2 ms^{-1}. Since QuikSCAT refers to equivalent neutral winds at 10 meters height, it can be argued that due to stability, it is not always representative of the real-time conditions. During spring and early summer months, frequent stable conditions will lead to an underestimation of the wind from QuikSCAT, which may be the reason for very frequent low winds that do not correspond to warming especially in the south Baltic sea and Skagerrak.

CONCLUSION

This study has shown that diurnal warming of the sea surface occurs in relatively high latitudes (more than 50^0 North), during the spring and summer months. Measurements from an infra-red radiometer are

limited by cloud coverage therefore data availability regulated our knowledge about the frequency of such events. The areas of most frequently observed events coincide well with areas of frequently observed low winds. These were areas of generally complex coastal morphology and high water turbidity, with the Baltic Sea exhibiting significantly more diurnal warming than the North Sea. Given the fact that the night-time reference fields hold an important role in the definition of day-time warming, an extended sensitivity analysis was performed. It was shown that measurements from SEVIRI can be successfully implemented in order to generate night-time reference fields, the performance of which matched the one of operationally available foundation temperature fields. On average, anomalies more than two degrees K were frequently observed, while anomalies of six degrees were also observed. Local time varied from 14:00 to 16:00 hours, with maximum number of cases being recorded at 15:00 (local times). The annual distribution of such events indicated that anomalies larger than one degree may occur throughout the year, most frequently observed from April to September. Anomalies larger than three degrees were constrained between April and August, while the maximum number of events occurred in June. This corresponded very well with the observed annual distribution of very low winds, for which observations peaked in June and the known solar insolation distribution that peaks during summer.

References

Cornillon, P, Stramma, L., (1985) The distribution of diurnal sea surface temperature events in the western Sargasso sea. J. Geophysical Research, **90**, C6, 1985, pp 11811-11815

Deschamps, P.Y., Frouin, R., (1984) Large Diurnal Heating of the Sea Surface Observed by the HCMR Experiment. J. Physical Oceanography, **14**, 1984, pp 177-184

Donlon, C., et al., (2007) The Global Ocean Data Assimilation Experiment High-resolution Sea Surface Temperature Pilot Project. Bull. American Meteorological Society, **88**, 2006, pp 1197-1213

Gentemann, C.L., et al., (2003) Diurnal signals in satellite seas surface temperature measurements. Geophysical Research Leters, **30**, 3, 2003, pp 1140-1144

Gentemann, C.L., et al., (2008) Multi-satellite measurements of large diurnal warming events. Geophysical Research Leters, **35**, L22602

Gentemann, C.L., Minnett, P.J., (2008) Radiometric measurements of ocean surface thermal variability. J. Geophysical Research, **113**, C08017

Hoeyer, J.L., She, J., (2007) Optimal Interpolation of sea surface temperature for the North Sea and Baltic Sea. J. Marine Systems, **65**, 2007, pp 176-189

Hoffman, R.N., Leidner, S.M. (2005) An introduction to the near-real-time QuikSCAT data. Weather and Forecasting, **20**, 2005, pp 476-493

Kaiser, J.A.C., (1978) Heat balance of the upper ocean under light winds. J. Physical Oceanography, **8**, 1978, pp 1-12

Merchant, C.J., et al., (2008) Diurnal warm-layer events in the western Mediterranean and European shelf seas. Journal, Geophysical Research Leters, **35**, L04601

Stramma, L., Cornillon, P., Weller, R.A., Price, J.F., Briscoe, M.G. (1986) Large diurnal sea surface temperature variability: satellite and in situ measurements. J. Physical Oceanography, **16**, 1986, pp 827-837

Stommel, H., et al., (1969) Observations of the diurnal thermocline. Deep-Sea Research, **16**, 1969, pp 269-284

Stuart-Menteth, A.C., et al., (2003) A global study of diurnal warming using satellite-derived sea surface temperature. J. Geophysical Research, **108**, C5, 3155, 2003

Ward, B., (2006) Near-surface ocean temperature. J. Geophysical Research, **111**, C02004.